Theoretical Reproduction of Fractional Quantum Hall Resistivity and Quasiparticle Energy Gaps

Jongbae Hong
Institute for Basic Science, Incheon National University, Yeonsu-gu, Incheon 22012, Korea
(Dated: December 15, 2024)

Experimental fractional quantum Hall resistivity and quasiparticle energy gaps are reproduced theoretically by considering correlated many-electron dynamics in incompressible strips under nonequilibrium transport. Plateau width and chemical potential are determined as well as plateau positions. Electrostatic confining potential of the incompressible strip causes deformed cycloidal electron motion. The confining potential is replaced by an image electron with the same spin, which gives rise to a composite boson of spin unity as a quasiparticle in describing current flow. Zeeman effect for the total spin of correlated quasiparticles further splits the Landau level, and forms the energy gaps and plateaus in Hall resistivity.

PACS numbers:

Two-dimensional (2D) electron systems often exhibit marvelous phenomena [1–3], with one being the fractional quantum Hall effect (FQHE) [2]. It is well known that in a clean system at low temperature, many plateaus are observed at various fractional LL filling ν in Hall resistivity. Even though the Laughlin wavefunction [4] provides the basic idea behind the effect and the composite fermion theory [5, 6] predicts most of the observed plateaus, a microscopic understanding of the FQHE has remained elusive. For example, neither plateau width nor the chemical potentials can be determined by these theories, and therefore, experimental Hall resistivity cannot be reproduced. In addition, the quasiparticle energy gaps, as fundamental quantities of the FQHE, call for more detailed explanation.

The purpose of this study is to reproduce an experimentally measured fractional quantum Hall (FQH) resistivity curve [7] and energy gaps [8] via the consideration of correlated many-electron dynamics in current flow, in which electron motion does not form a closed orbit. This point of view may provide new insights into this profound subject. To this end, essential pieces of information are where and how the Hall current flows. Halperin [9] first proposed electron flow in the edge due to Landau level (LL) bending. Early studies on edge current can be found in [10, 11]. However, previous studies on current flow were unsuccessful. Several years ago, experiments measured Hall voltage profiles across the Hall bar of an integer quantum Hall (IQH) system using a scanning probing microscope [12], which showed that Hall current flows in both edge and bulk regions. The same result has been observed by microwave impedance microscopy [13]. Recently, the above-mentioned scanning probing microscope group observed similar Hall current features for an FQH system of filling factor 2/3. These experiments and theoretical studies [14, 15] argue that there are incompressible strips in the region of edge, through which the Hall current flows.

In this study, we consider an FQH system with fully polarized electrons occupying the lowest LL (LLL), i.e. $\nu \leq 1$, as shown in Fig. 1(a). Two incompressible strips (yellow) are depicted, with LL bending according to [12–15]. We did not draw the incompressible bulk region explicitly in Fig. 1(a) because the incompressible strips are wide enough to show the features of current flow in the incompressible bulk.

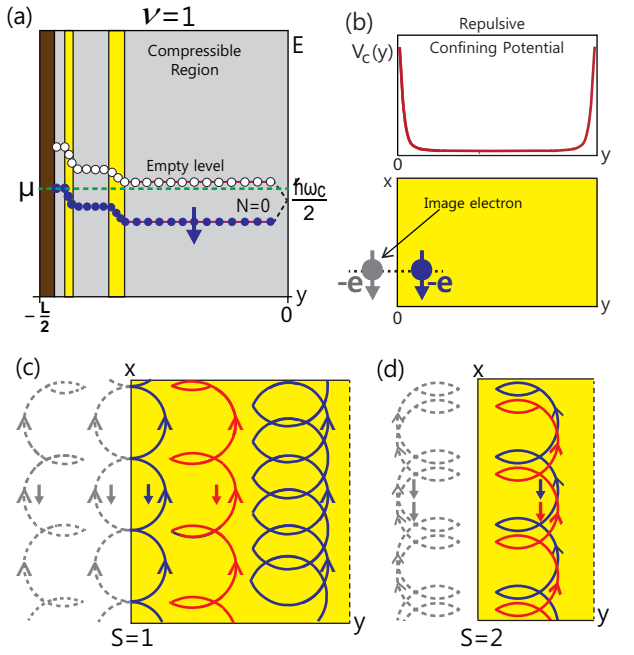

FIG. 1: (a) Schematic of the energy spectrum of the LLL for $\nu = 1$ in the left half of a Hall bar of width L. Two incompressible strips (yellow), a depletion region (brown), and compressible regions (grey) are presented. We adopt a negative g factor [16], and μ denotes the chemical potential. (b) (upper panel) Repulsive confining potential in the incompressible strip shown in (a). (lower panel) An image electron (grey) replaces the confining potential along with a real electron (blue) with the same spin. (c) Current dynamics in the incompressible region: skipping and cycloid-type motions of an electron and its image. The quasiparticle has spin $S = 1$. The rightmost depicts cycloid-type motion in a weaker confining potential. (d) Skipping motion of two correlated electrons and their images forming total spin $S = 2$.

Semiclassical electron trajectory in an incompressible strip is a slightly deformed cycloid attributed to the electrostatic confining potential at the strip's boundary, although it is not explicitly shown in calculations using a simplified model [14] or the Thomas–Fermi approximation [15]. We expect that this confining potential may be shown if many-electron correlation is fully taken into account. In the upper panel of Fig. 1(b), we sketch the confining potential; this potential is then replaced by an image electron with the same spin shown in the lower panel in Fig. 1(b), thereby securing that the wavefunction will not leak out of the incompressible region due to the Pauli principle.

In Fig. 1(c), we illustrate three possible trajectories of an electron and its image in an incompressible strip: skipping, deformed cycloid, and slower one (without drawing its image motion) depending on the position of electron. An electron and its image behave as a quasiparticle with a spin state of $|\chi_{\downarrow\downarrow}\rangle$ indicating total spin $S = 1$. We choose negative g factor [16]. Therefore, a quasiparticle formed in current flow is a composite boson. The role of many-body interaction in Fig. 1(c) is to construct the confining potential.

Next, we consider many-body correlation among flowing electrons, which causes correlated multi-quasiparticle motion. We sketch a correlated two-quasiparticle motion in Fig. 1(d), but note that many other types are possible. The spin state of two correlated composite bosons is written as $|\chi_{\downarrow\downarrow\downarrow\downarrow}\rangle$ with total spin $S = 2$. One can easily imagine correlated three-quasiparticle motion ($S = 3$) and more multi-quasiparticle motions by the same manner.

The Hamiltonian for the incompressible region of a Hall bar is composed of a term for the LLs, Zeeman splitting for individual electrons, confining potential $V_C(y)$, and inter-electron interaction $U(x, y)$. The latter two are replaced by the Zeeman term for correlated composite bosons, and Coulomb interaction between the electron and its image is neglected because of the strong magnetic field Thus, the Hamiltonian is written as

$$H = \frac{\sum_i (\vec{p}_i + e\vec{A}_i)^2}{2m_0} - g^*\mu_B \frac{\vec{s}}{\hbar}\cdot\vec{B} - \sum_{n=1}^{\infty} g_n^{cb}\mu_{Bn}^{cb}\frac{\vec{S}_n}{\hbar}\cdot\vec{B}, \quad (1)$$

where m_0 is bare electron mass, $\vec{p}$ and $\vec{A}$ are electron momentum and vector potential, respectively, g^* is the effective Landé g factor in the Hall bar, $\mu_B = e\hbar/2m_0$ is the Bohr magneton where $\hbar = h/2\pi$ with Planck constant h, $\vec{s}$ is the spin operator of an electron, and g_n^{cb}, μ_{Bn}^{cb}, and $\vec{S}_n$ are respectively the g factor, Bohr magneton, and total spin operator of correlated n composite bosons. Thus, $\mu_{Bn}^{cb} = e\hbar/2m_n^{cb}$ with mass of a composite boson m_n^{cb} under n-quasiparticle correlation, and $g_n^{cb}\mu_{Bn}^{cb} = \sum_i (g_{n,i}^{cb})(\mu_{Bn,i}^{cb})$, where $\sum_i$ denotes the sum over all different types of deformed cycloidal motion.

The Hamiltonian in Eq. (1) is easily diagonalizable. Setting $\vec{B} = B\hat{z}$ gives $S_n^z|\chi\rangle = j_n\hbar|\chi\rangle$, where $j_n = -n, \cdots, 0, \cdots, n$ for integral spin value $S_n = n$. Thus, the energy eigenvalues for a given filling factor ν are given by

$$E_{N,\sigma,j}^{\nu} = \hbar\omega_c(N + 1/2 - \zeta\sigma - \sum_n \delta_n^{\nu} j_n), \quad (2)$$

where $\omega_c = eB/m_c^*$ with m_c^* the cyclotron effective mass, $N = 0, 1, 2, \cdots$, $\zeta = (g^*/4)(m_c^*/m_0)$, $\sigma = \pm 1$, and $\delta_n^{\nu} = (m_c^* g_n^{cb}/2m_n^{cb})^{\nu}$. The values of δ_n^{ν} represent the degree of n-quasiparticle correlation for a given ν, which will be determined in the process of fitting Hall resistivity and the energy gaps.

FQH resistivity can be attained by considering classical Hall resistivity, $\rho_{xy} = B/e\rho_c$, in a quantum mechanical manner. The carrier density ρ_c is the density of electrons in the incompressible regions formed in both edge and bulk [12, 13], and it is given by counting the quantum states determined by N, σ, and j below the chemical potential. Since both chemical potential and energy eigenvalues depend on filling factor ν, the Fermi distribution function also depends on ν. Therefore, FQH resistivity ρ_{xy} must be obtained separately for each plateau region by performing a state sum for the Fermi distribution function, i.e. $\rho_{xy}^{\nu} = (B/e)[\sum_k f^{\nu}(E_k)]^{-1}$. In this study, since we consider only $\nu \leq 1$, the state sum for the Fermi distribution function is written as

$$\sum_k f^{\nu}(E_k) = D_L \sum_{\{j\}} \frac{1}{1 + \exp[\beta(E_{0,\sigma=-1,j}^{\nu} - \mu^{\nu})]}, \quad (3)$$

where $D_L = eB/h$, $\beta = 1/k_B T$, and the expression of energy eigenvalues is given in Eq. (2). For considering up to three-particle correlation, e.g., the sum $\sum_{\{j\}}$ is

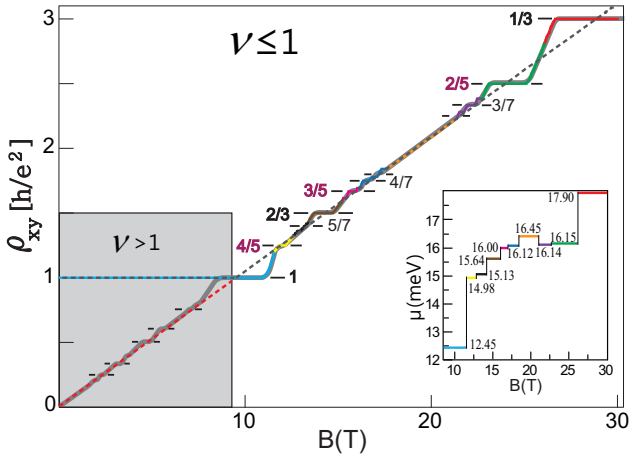

FIG. 2: Theoretical FQH resistivity is superimposed on the experimental data given in [7]. The grey dashed line represents the full orange line, and the red dashed line is an extension of the grey. The chemical potentials in the inset are matched to the Hall resistivity line according to color.

given by $\frac{1}{3\cdot5\cdot7}\sum_{j_1=-1}^{+1}\sum_{j_2=-2}^{+2}\sum_{j_3=-3}^{+3}$, where the front factor is introduced to secure Fermi distribution function unity for the occupied states. A similar expression is given in [17].

In Fig. 2, we plot our theoretical FQH resistivity for $\nu \leq 1$ superimposed on the experimental data reported in [7]. In obtaining Fig. 2, we use $m_c^*/m_0 = 0.067$ of GaAs and $g^* = -0.18$ [16], which give $\hbar\omega_c = (1.73\text{meV/T})B$ and $\zeta = -0.003$, respectively. We calculate at temperature $T = 10$ mK using the values of δ_n^ν given in Table I and chemical potentials given in the inset of Fig. 2. Hall resistivity and chemical potential are matched by the same colors. Agreement with the experimental data (grey) is nearly perfect.

Interesting discoveries in Fig. 2 are the step-wise behavior of chemical potential indicating the incompressible nature of the plateau state and the Fermi liquid feature [18] of the orange section around $\nu = 1/2$, as shown by the grey and red dashed lines. We reveal that plateau width is mostly determined by the degrees of two- and three-quasiparticle correlations represented by δ_2 and δ_3: one can see similar values of δ_1 in Table I. The relatively small value of δ_4, representing four-quasiparticle correlation, smooths out the Hall resistivity curve. These δ_n vanish one-by-one from larger n, and accordingly the FQHE plateaus, as disorder increases. Thus, the FQH system changes into an IQH system at a certain level of disorder, where even skipping orbit is broken, but chirality is retained [19]. The values of δ_n though are not fully determined by fitting the Hall resistivity curve alone. But simultaneous fitting of both Hall resistivity and the energy gaps fix δ_n. Hence, we naturally look to the issue of quasiparticle energy gaps.

Energy gaps in the FQHE are basically formed by a splitting of the LL. The lowest order splitting occurs from the formation of a single quasiparticle of total spin $S = 1$, which yields three energy eigenstates corresponding to $S^z = 1$, $S^z = 0$, and $S^z = -1$ under a magnetic field. These eigenstates are separated by δ_1, as shown in Fig. 3, and each state has degeneracy $D_L^{(1)} = eB/3h$, implying that a composite boson behaves as if it has a fractional charge of $e/3$ in transport under a Hall bias. Formation of an $S = 1$ quasiparticle yields major plateaus at filling factors $p/3$, where p denotes positive integers not larger than the denominator.

Higher-order LL splitting follows correlated multi-quasiparticle dynamics. Two correlated composite bosons have total spin $S = 2$, and yield five energy eigenstates separated by δ_2. At this level of the splitting hierarchy, the second major plateaus appear at $\nu = p/5$. Plateaus at $\nu = p/7$ appear in the next stage by three correlated composite bosons of total spin $S = 3$, which further separates each state into seven by δ_3, as shown in Fig. 3. This type of hierarchy was previously proposed in [17], without specific dynamics. We neglect the separation by δ_4 in obtaining the present energy gap.

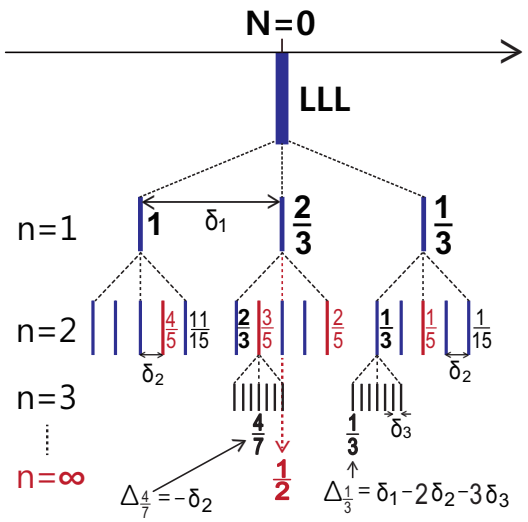

FIG. 3: Dimensionless parts of quasiparticle energy gaps, Δ_ν, are caused by further LL splitting. We explicitly show $\Delta_{1/3}$ and $\Delta_{4/7}$ considering up to $n = 3$. The gapless nature of $\nu = 1/2$ state is clarified in the limit of the splitting hierarchy.

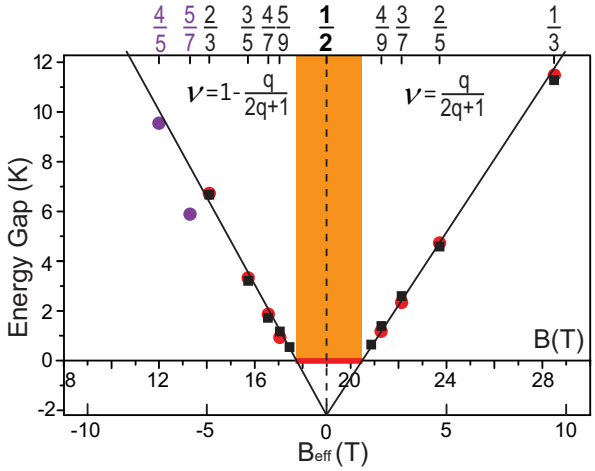

FIG. 4: Theoretical quasiparticle energy gaps (red circles) obtained via $E_g^\nu = (0.671\text{K/T})(m_0/m_{cb})2|\Delta_\nu| \cdot |B_\nu - B_{1/2}|$ with $m_{cb}/m_0 = 0.21$ superimposed on experimental data (black squares and fitting lines) [8]. Filling factors are located on the upper horizontal axis. The violet circles belong to a different sequence.

All odd-denominator filling factors existing in the $\nu \leq 1$ region appear as the splitting hierarchy continues down. We classify the odd-denominator filling factors by considering $\nu = 1/2$ state as the Fermi level [18]. The zero-gap state of $\nu = 1/2$ is clarified in the limit $n \to \infty$ in Fig. 3. Then, particle states are given by the sequences $\nu = q/(2q+1)$, $\nu = q/(2q+3)$, $\nu = q/(2q+5)$, $\cdots$ where $q = 1, 2, \cdots$, and hole states are $\nu = 1 - p/(2p+1)$, $\nu = 1 - q/(2q+3)$, $\nu = 1 - q/(2q+5)$, $\cdots$. These cover all odd-denominator filling factors observed in the region $\nu \leq 1$ [20].

TABLE I: **Values of δ_n, dimensionless gap Δ_ν, and $B_{\rm eff}$(T).**

Color	Red	Green	Violet	Orange	Blue	Magenta	Brown	Black	Yellow	Cyan
ν	1/3	2/5	3/7 (4/9)*	1/2	(5/9)* 4/7	3/5	2/3	5/7	4/5	1
δ_1	0.296	0.30	0.305	0.335	0.302	0.28	0.28	0.253	0.253	0.123
$\delta_2(\times 10^{-1})$	0.48	0.82	0.99	0.67	1.21	1.0	1.0	0.48	0.57	0.11
$\delta_3(\times 10^{-2})$	0.35	0.29	1.86	0.96	4.6	2.0	0.5	0.57	0.57	0.45
$\delta_4(\times 10^{-3})$	0.5	0.5	0.3	1.0	0.5	0.5	0.5	0.2	0.2	0.2
Δ_ν		$2\delta_2-3\delta_3$	$\delta_2+\delta_3$		$-\delta_2$	$-\delta_2-3\delta_3$	$-2\delta_2-3\delta_3$			
$\lvert B_\nu - B_{\frac{1}{2}}\rvert$	9.5	4.75	3.12 (2.25)		(1.99) 2.43	3.29	4.9	5.7	7.0	

$\Delta_{4/9}=\delta_2-\delta_3-\delta_4$, $\Delta_{5/9}=-\delta_2+\delta_3+2\delta_4$, $\Delta_{5/7}=-\delta_1+2\delta_2-\delta_3$, and $\Delta_{4/5}=-\delta_1+\delta_2-3\delta_3$.
For $\nu=4/9$ (5/9), we use δ_n of $\nu=3/7$ (4/7) in obtaining energy gap in Fig. 4.

According to the IQHE, energy gap is composed of the dimensionless part $(N+1/2)$ and $\hbar\omega_c$. In Fig. 3, we show how the dimensionless part in FQHE, Δ_ν, is given in terms of δ_n. $\Delta_{1/3}$ and $\Delta_{4/7}$ are explicitly presented as examples, with other Δ_ν given in Table I. We introduce a new energy scale for a composite boson quasiparticle as $\hbar\omega_{cb}=\hbar eB_{\rm eff}/m_{cb}$, where m_{cb} is the cyclotron effective mass of a composite boson. Thus, one can write the quasiparticle energy gap at filling factor ν as $E_g^\nu=\hbar\omega_{cb}^\nu|\Delta_\nu|$, where $\omega_{cb}^\nu=(e/m_{cb})|B_\nu-B_{1/2}|$. We plot E_g^ν (red circles) in Fig. 4 using $m_{cb}/m_0=0.21$. The experimental data (black squares and solid lines) provided in [8] are superimposed for comparison, and the agreement is perfect.

Our understanding of Fig. 4 is somewhat different from the explanation given in [6, 8, 21]. We believe that a gapless region may indeed exist, and that it covers the region indicated by the red bar or orange area ranging out to the two points where the linear lines meet the zero gap line. The violet circles at $\nu=5/7$ and 4/5 in Fig. 4 belong to the hole state sequence $\nu=1-q/(2q+3)$. More experimental data on energy gaps are needed to discuss the different classes of filling factor sequences.

In conclusion, we reproduced experimental FQH resistivity and energy gaps for $\nu\le 1$ via the consideration of many-body correlations in electron transport in an incompressible strip in which electrons perform deformed cycloidal motions due to the confining potential. This situation is described by correlated composite bosons having integral spins. The Zeeman splitting for the correlated composite bosons is responsible for the essential features of the FQHE. The $\nu>1$ region which we excluded in this work contains spin transitions to higher LLs and encounters the even-denominator filling factor $\nu=5/2$; therefore, $\nu>1$ may present more challenging and attractive studies.

The author appreciates J. Weiss, A. Gauss, R. Haug, and T. Toyoda for their valuable discussions and help. This work was supported by Project Code (2017R1D1A1A02017587) and partially supported by a KIAS grant funded by the MSIP.

[1] K. von Klitzing, G. Dorda, and M. Pepper, Phys. Rev. Lett. **45**, 494 (1980).
[2] D. C. Tsui, H. L. Stormer, and A. C. Gossard, Phys. Rev. Lett. **48**, 1559 (1982).
[3] J. G. Bednorz and K. A. Müller, Zeit. für Phys. B **64 (2)**, 189 (1986).
[4] R. B. Laughlin, Phys. Rev. Lett. **50**, 1395 (1983).
[5] J. K. Jain, Phys. Rev. Lett. **63**, 199 (1989).
[6] J. K. Jain, *Composite Fermions* (Cambridge Univ. Press, Cambridge, 2007).
[7] J. P. Eisenstein and H. L. Stormer, Science **248**, 1510 (1990).
[8] R. R. Du, H. L. Stormer, D. C. Tsui, L. N. Pfejffer, and K. W. West, Phys. Rev. Lett. **70**, 2944 (1993).
[9] B. I. Halperin, Phys. Rev. B **25**, 2185 (1982).
[10] R. J. Haug, Semicond. Sci. Technol. **8**, 131 (1993).
[11] M. Büttiker, Phys. Rev. B **38**, 9375 (1988).
[12] J. Weiss and K. von Klitzing, Phil. Trans. R. Soc. A **369**, 3954 (2011).
[13] K. Lai, W. Kundhikanjana, M. A. Kelly, Z.-X. Shen, J. Shabani, and M. Shayegan, Phys. Rev. Lett. **107**, 176809 (2011).
[14] D. B. Chklovskii, B. I. Shklovskii, L. I. and Glazman, Phys. Rev. B **46**, 4026 (1992).
[15] K. Lier and R. R. Gerhardts, Phys. Rev. B **50**, 7757 (1994).
[16] M. J. Snelling, G. P. Flinn, A. S. Plaut, R. T. Harley, A. C. Tropper, R. Eccleston, and C. C. Phillips, Phys. Rev. B **44**, 11345 (1991).
[17] T. Toyoda, Sci. Rept. **8**, 12741 (2018).
[18] B. I. Halperin, P. A. Lee, and N. Read, Phys. Rev. B **47**, 7312 (1993).
[19] C. W. J. Beenakker and H. van Houten, Solid State Phys. **44**, 1 (1991).
[20] W. Pan, J. S. Xia, H. L. Stormer, D. C. Tsui, C. Vicente, E. D. Adams, N. S. Sullivan, L. N. Pfeiffer, K. W. Baldwin, and K. W. West, Phys. Rev. B **77**, 075307 (2008).
[21] H. L. Stormer, D. C. Tsui, and A. C. Gossard, Rev. Mod. Phys. **71**, S298 (1999).